

Received: 2014.12.20
Accepted: 2015.01.13
Published: 2015.05.26

Development of Femoral Head Interior Supporting Device and 3D Finite Element Analysis of its Application in the Treatment of Femoral Head Avascular Necrosis

Authors' Contribution:

Study Design A
Data Collection B
Statistical Analysis C
Data Interpretation D
Manuscript Preparation E
Literature Search F
Funds Collection G

ABCDEF Dongmin Xiao
BCDEF Ming Ye
CDEF Xinfa Li
CEF Lifeng Yang

Department of Orthopedics, Hunan Provincial Yongzhou Central Hospital
(Affiliated Yongzhou Hospital of Nanhua University), Yongzhou, Hunan, P.R. China

Corresponding Author: Dongmin Xiao, e-mail: dr_dm Xiao@163.com
Source of support: Departmental sources

Background: The aim of this study was to develop and perform the 3D finite element analysis of a femoral head interior supporting device (FHISD).





Material/Methods: The 3D finite element model was developed to analyze the surface load of femoral head and analyze the stress and strain of the femoral neck, using the normal femoral neck, decompressed bone graft, and FHISD-implanted bone graft models.

Results: The stress in the normal model concentrated around the femoral calcar, with displacement of 0.3556 ± 0.1294 mm. In the decompressed bone graft model, the stress concentrated on the femur calcar and top and lateral sides of femoral head, with the displacement larger than the normal (0.4163 ± 0.1310 mm). In the FHISD-implanted bone graft model, the stress concentrated on the segment below the lesser trochanter superior to the femur, with smaller displacement than the normal (0.1856 ± 0.0118 mm).

Conclusions: FHISD could effectively maintain the biomechanical properties of the femoral neck.

MeSH Keywords: **Biomechanical Phenomena • Femur Head Necrosis • Finite Element Analysis**

Full-text PDF: <http://www.medscimonit.com/abstract/index/idArt/893354>

 2968  —  3  19



Background

There are many treatment methods towards the adult avascular necrosis, but the effects are unsatisfactory, and hip replacement would eventually be required. However, the artificial joint replacement has shortcomings such as infection, loosening, and abrasion. Because of the life restriction of artificial joints, multiple replacements would be required, especially in younger patients. Therefore, the current treatment of the disease is mainly focused on how to delay the replacement of artificial hip joints [1]. Therefore, a femoral head interior supporting device (FHISD) was developed, aiming to support the femoral head or reset the collapsed femoral head. Bone graft was also made below the femoral head and around the inner supporting device, hoping to achieve not only restoration of the mechanical properties of the femoral neck, but also conduct the fusion of the femoral neck bone graft, and not obstruct the future artificial joint replacement.

In this study, the finite element analysis was introduced through controlling experimental conditions such as finite elements, nodes, and DOF, to simulate the situation of human body mechanics, and perform biomechanical research on the FHISD treatment of avascular necrosis.

Material and Methods

Development of FHISD

Medical titanium alloy was used to make FHISD (Figure 1), including the following parts: top cover, supporting leaf, inner stem, top cap, sealing sleeve, and bottom cap.

Top cover: the top part was of hemispherical shape, and the lower part was a plane. In the center of the plane, there was a stud bolt, which was designed to match the hole in the inner stem. The top cover could be tightened on the upper part of

the inner stem, making the top of FHISD appear as a spherical curve, easy for the reset and supporting of the femoral head.

Supporting leaf: similar with fan-shape, with protruding edges in its center for the articulation with the hinged branches of inner stem. There were pin holes in the protruding edges, matching the pin holes on the hinged branches of inner stem. The distracted 3 supporting leaves would form a circle like an umbrella, the upper surface of the proximal end of the supporting leaf had shallow groove, which would coincide with the corresponding parts of top cover when the supporting leaf was distracted, and therefore prevent the over-distracted and form a smooth ball arc with top cover, increasing the head area of FHISD. When distracted, there were gaps among the leaves, benefiting for the bone grafting under the femoral head. The sizes of the leaves could be divided into large, medium, and small types, and could be selected according to the necrotic size of the femoral head.

Inner stem: a hollow prism-cylinder, with linkage-screw holes in its central planes of the upper and lower ends. On the upper plane of the inner stem, there were hinge grooves and corresponding pin holes for mounting the 3 supporting leaves, and the supporting leaves could spread around the stem. There was screw thread on the surface of inner stem, providing the movability of the top cap and the sealing sleeve. The hollow diameter was 2 mm, making it possible for the inner stem to be implanted into the lesion site along the direction of the Kirschner wire. According to need, the length of the inner stem could be 60–110 mm, with diameter 6–8 mm, or the inner stem could be divided into 2 parts, which would be easy to remove when replacing the joint in future.

Top cap: with internal threads, matching with the inner stem, the tightened top cap could distract the supporting leaves out.

Sealing sleeve: with internal threads, matching with the inner stem, and equipped with outer threads which could be used to

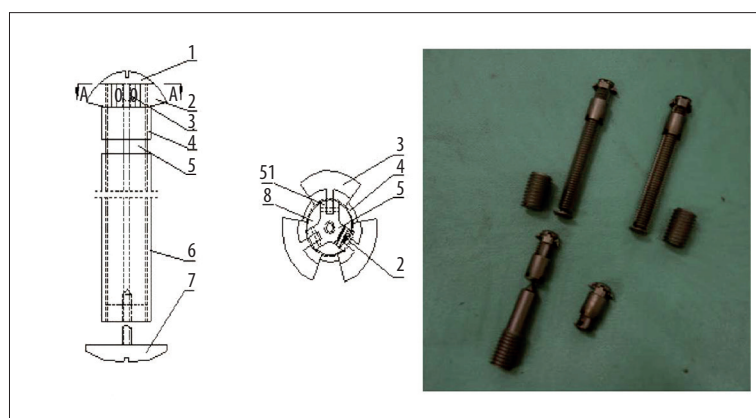


Figure 1. FHISD, including the following parts: top cover (1), supporting leaf (2), inner stem (3), top cap (4), column (5), sealing sleeve (6), bottom cap (7), interval (8), and branches (51).

screw into the bone tunnel, simulating the effects of pressing tight on the bone graft and preventing the sinking of the FHISD.

Bottom cap: a cover with a central stud bolt, which matched with the bottom screw hole of the inner stem, simulating closing the outside stoma of the tunnel.

When in use, the top cover would be fixed on the top of the inner stem; under the top cover were the supporting leaves, connecting with the inner stem through the hinge grooves; below the leaves were the top cap and the sealing sleeve, covering the inner stem; the bottom cap was located under the sealing sleeve.

Establishment of the femur experimental models

According to experimental purposes, 3 kinds of experimental models were established:

The normal femoral neck model: normal femoral neck specimen without any preparation.

The decompressed bone graft model: a 1-cm diameter tunnel was drilled from the femoral head center, along the lower edge of the lateral tuberosity of femur, to the 0.5 cm position below the femoral cartilage. Then a curette was used to scrape a space under the femoral cartilage, with the diameter about 2 cm (similar to the space left after the clearance of femoral head necrotic lesions), and then performed the bone graft.

FHISD-implanted bone graft model: following the method of the decompressed bone graft model, the femoral neck tunnel and femoral subchondral space were performed first, and then installed the FHISD into the decompressed tunnel, with the top cover reaching the space roof, then tightened the top cap to distract the supporting leaves like an umbrella, then performed the bone graft into the space between the supporting leaves and the bone tunnel, screwed the sealing sleeve to press the bone graft close and fixed the FHISD, tightened the bottom cap and closed the tunnel outer stoma.

Establishment of the 3D finite element model

The 3 models were performed in the 64-row CT Thin-Layer Scan. The cross-sectional scanning was performed from the proximal end to the distal end of the femoral head, perpendicular to the longitudinal axis, with the layer thickness and layer space both as 0.5 mm. The scan data processed with interpolation and amplification would generate a 0.5 mm-thick continuous cross-sectional image. The image file was then transferred from the CT processing workstation into the computer for 3D reconstruction. After the image conversion, the data was then imported as the Dicom format into Mimics software

for grayscale threshold adjustment and regional segmentation to establish the 3D finite element models towards the above 3 models established.

The normal femoral model and the FHISD model were imported, as the STL format, into the Freeform software. Referring to the clinical practice, the FHISD was assembled on the normal femoral model, defining the relationship of FHISD and femur as the binding, and fixed without any looseness.

In Freeform software, the surfacing treatment results of the models were imported as the IGES format into Ansys finite element analysis software, with the shell63 element used to simulate the regional cortical bone above the femoral neck, and the other structures used 10-nodes-solid92 unit for the mesh partition.

The basic information and stress of the 3 models were recorded to draw their stress cloud, respectively, and the stress distribution curves were also drawn according to a series of nodes stress values taken along the lateral femoral neck (from the top of the femoral neck and along the direction of femoral neck) and the medial femoral neck (from the lower of the femoral neck and along the direction of femoral neck), the stress distribution of the femoral neck was then analyzed; meanwhile, according to the displacement values of the femur after stress loading, the displacement contour was drawn for the analysis of the femoral strain situation after stress loading.

Loading and boundary conditions

The surface loading that acetabula forced on the femoral weight-bearing area when standing on one leg was stimulated. The nodes in about 36 mm range of femoral head were selected to simulate the contact surface with the acetabulum, uniformly distributed loading was applied along the normal direction of the nodes, making the resultant force acting on the femoral head point at the centroid of the femoral head, with the amount as 2100 N, and the angle direction of the resultant force was 25° to the long axis of the femoral head.

Results

The FHISD has obtained Chinese new utility model patents (Patent No. ZL20072 0062263.0).

Stress results after loading

Stress cloud of the normal femoral neck model (Figure 2A)

Based on the measured basic information in the normal femoral neck model and the stress cloud plotted with the stimulated

stress loading, the normal stress of femoral head and neck when loaded concentrated on the femoral calcar, the max value was $637\text{E}+08$ (637×10^8) Pascal; and the stress gradually decreased towards around and transferred to the proximal end of femur from max stress center.

Stress cloud of the decompressed bone graft model (Figure 2B)

Because the cancellous bone, implanted into the tunnel after the decompressed bone grafting, had little difference in terms of organs and structures with the normal femoral neck model, so the elastic modulus and the Poisson's ratio were almost the same as the normal, the stress cloud displayed that the stress concentrated on the region in the medial part of the femoral head and neck, which was equivalent to the femoral calcar, the max value was $666\text{E}+08$. Based on this center, the stress descended towards the surrounding in the manner of concentric circles; because of the existence of the bone tunnel in the decompressed bone graft model, we found that the stress concentrated on the anterolateral part of the femoral head, and the stress value on the top of the femoral head was larger than the normal, with wider range, and its value was $223\text{E}+08$, the stress under the medial part of the femoral head was larger than the normal, and the value was $755\text{E}+08$, the stress under the lesser trochanter was larger than the normal, with the value as $149\text{E}+08$, and the stress on the femoral shaft was the minimal.

Stress cloud of the FHISD-implanted bone graft model (Figure 2C)

After the implantation of the FHISD, the stress transferred directly through the FHISD from the femoral head to the trochanter, so the stress on the femoral head was less, while the stress under the lesser trochanter was greater, with the max value as $299\text{E}+08$; at the same time, the FHISD had a higher stress, while no stress concentrated on the femoral head and neck, the stress value was small as about $408\text{E}+07$; thus, the stress of the femoral head in the FHISD-implanted bone graft group was significant less than the decompressed bone graft group, no stress concentrated, meanwhile, the FHISD was observed to burdensome stress.

Displacement results after stress loading

In the normal femoral head group, the displacement increased starting from the greater trochanter towards the direction of the femoral head, the max displacement appeared on the femoral head, with the value as 0.632 mm, and the smallest displacement was on the greater trochanter, with the value as 0.0141 mm, the displacement average value was 0.3556 ± 0.1294 mm (Figure 3A).

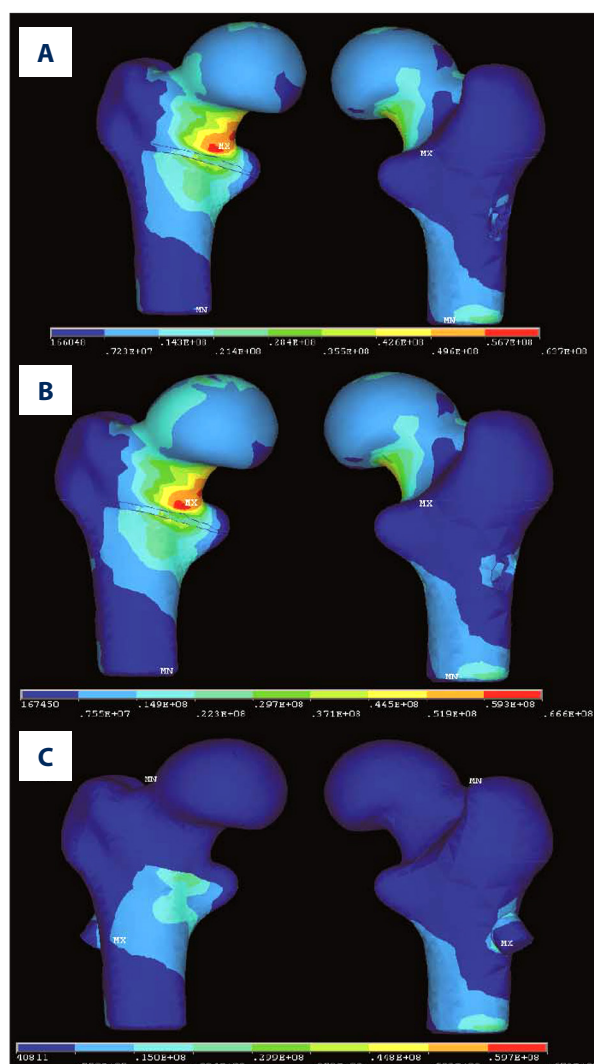


Figure 2. (A) Stress cloud of the normal femoral neck model, the max stress value was in the red zone. (B) Stress cloud of the decompressed bone graft model, the max stress concentrated on the top of the femoral head. (C) Stress cloud of the FHISD-implanted bone graft model, there is no obvious stress concentration on the femoral neck.

In the decompressed bone graft group, the displacement increased starting from the greater trochanter towards the direction of the femoral head, the max displacement appeared on the femoral head, with the value as 0.682 mm, and the smallest displacement was on the greater trochanter, with the value as 0.026 mm, the displacement average value was 0.4163 ± 0.1310 mm. It could be seen that the displacement in the decompressed bone graft group was bigger than the normal group, and the strain was also larger (Figure 3B).

In the FHISD-implanted bone graft group, the displacement increased starting from the greater trochanter towards the direction of the femoral head, the max displacement appeared

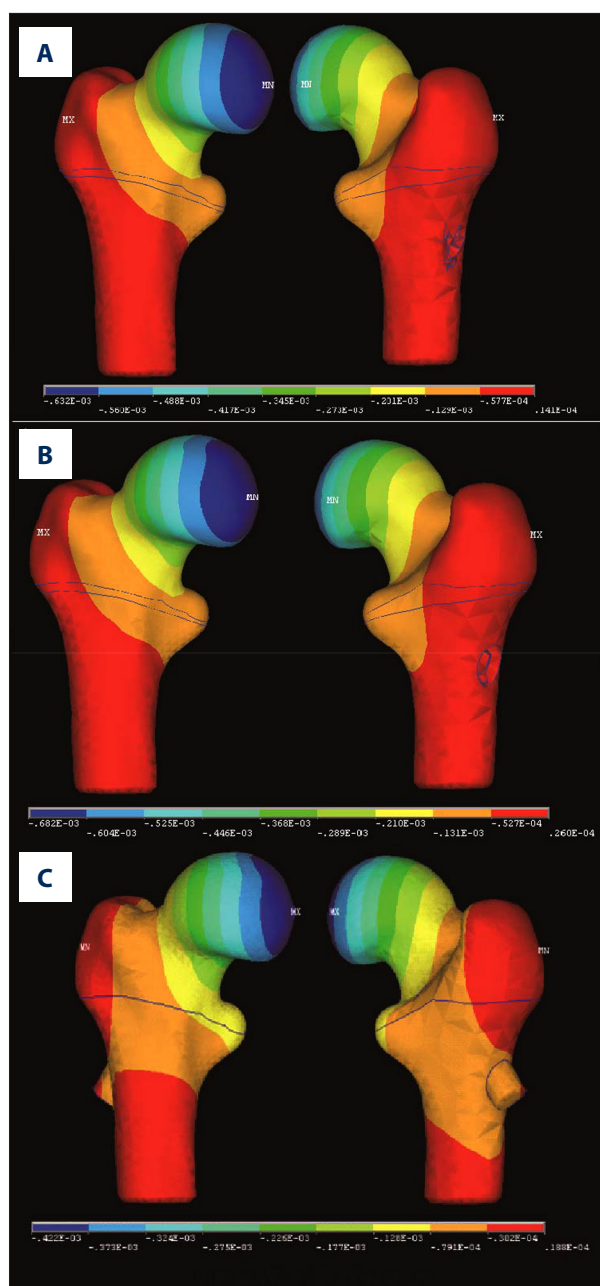


Figure 3. (A) Displacement cloud of the normal femoral neck model. (B) Displacement cloud of the decompressed bone graft model. (C) Displacement cloud of the FHISD-implanted bone graft model.

on the top of femoral head (0.422 mm), and the smallest displacement was on the greater trochanter and the femoral shaft (0.0188 mm), the displacement average value was 0.1856 ± 0.0118 mm, less than the normal group, indicating the strain was small (Figure 3C).

Discussion

The treatment of femoral head necrosis is currently a problem in orthopedics; the treatment methods are non-surgical treatment and surgical treatment. The non-surgical treatment methods include drug therapy, mainly using vasodilators. Shockwave adjuvant therapy, hyperbaric oxygen therapy, and various approaches that use growth factors to promote the regeneration of blood vessels and new bone formation in the repairing process have made remarkable achievements in the treatment of avascular necrosis [2–8]. Surgery is the main method in the treatment of avascular necrosis. The various surgical methods each have advantages and disadvantages and the specific choice mainly depends on the severity and the patient's age. The usual surgical methods are bone transplantation, bone marrow transplantation, vascular grafts, femoral reconstruction, pith decompression, and artificial hip replacement [1,9–15].

The various treatment methods have certain advantages and disadvantages. The ideal treatment method should not only be able to effectively improve the blood supply towards the femoral head and promote the repair of necrotic bone, but also be able to improve the mechanical properties of the femoral head and to prevent the collapse of the femoral head [9]. Normally, the case develops to the collapse situation or the existing collapse further aggravates, leading to the eventual hip arthroplasty. Therefore, it is very important to effectively prevent the occurrence and development of femoral head collapse, to promote the regeneration of new bone, and to restore the biomechanical properties [10].

We developed a FHISD to support the femoral head or to reset the collapsed femoral head, and to perform the bone graft under the femoral head and around the FHISD, which would finally help to restore the mechanical properties of femoral head and neck and the graft fusion in the femoral head and neck, while not harming the artificial hip replacement in future. This is a new treatment of adult avascular necrosis of the femoral head. We developed supporting leaves that can open and close along the axis of the inner stem, then implanted it into the necrotic decompressed site through a small decompressed tunnel to support the femoral head or reset the collapsed femoral head. The supporting leaves can be opened like an umbrella, expanding the top cover area of the FHISD and increasing the support area towards the femoral head. The prism-cylinder structure allows performing the bone graft under the top cover and around the inner stem. The FHISD was fixed into the bone tunnel with the external thread of the sealing sleeve, which strengthens its anti-sinking ability and prevents collapse. This method allows minimally invasive surgery for avascular necrosis and prevents postoperative re-collapse.

In the experiment, we performed 64-row spiral CT tomography on the 3 experimental models. The images were then imported in Dicom format into Mimics software. After grayscale threshold adjustment and regional segmentation, the finite element model was reconstructed, so the accuracy of the simulation could be significantly improved, and the physical geometric simulation would be much closer to the real situation, with high emulating characteristics. For simplicity, the bone tissue was considered equivalent as a whole material, among which the elastic modulus of cortical bone, cancellous bone, cartilage layer, and Ti were 1×10^{10} , 5×10^8 , 1×10^7 , and 1.13×10^{11} , respectively. The 2 parameters – stress and displacement (strain) – were set for the 3 models, then the cloud graph and cure graph were drawn depending on the relative values for the changes analysis. From the stress cloud of the normal femoral head model, it could be seen that the calcar had stress concentration, with the cortical bone as the thickest and the highest-density part, which could withstand the high stress formed by the upper body weight, while without fracture, this stress and bone density distribution fit Wolff's law. At the same time, the stress decreased around along the calcar-centered concentric circles; after stress loading, the displacement decreased from the femoral head to the femoral shaft, which was relevant to the elastic modulus, material structure, the force, and the force-receiving part. Under the same force, the larger the elastic modulus, the smaller the deformation and the smaller the displacement (i.e., the smaller the strain, which could simply reflect the buffer capacity of the specimen). From the finite element cloud of the decompressed bone graft model, we observed that because the implanted cancellous bone had the same elastic modulus as those in the normal femoral head and neck, the stress cloud had little difference from the normal model, but the stress increased, and the range became wider, leading to mechanical structural changes of the tunnel.

Although the cancellous bone was implanted, it did not provide good support, so the displacement increased, and the strain became greater. From the FHISD-implanted bone graft cloud model, we found that the stress value of the entire femoral head decreased, the stress of the femoral head passed down through the FHISD and focused mainly on the femoral proximal part, the displacement was smaller than normal (related to the stress load transmission onto the FHISD) spread and dispersed along the supporting leaves, and kept on passing down along the inner stem. Though the elastic modulus of Ti was significantly different from the bone tissues, the FHISD effectively reduced the pressure on the femoral head, and reduced the displacement of the femoral head after compressed, providing better support. Therefore, the tunnel decompression and bone graft clinically reduced the bone pressure, removed the dead bone tissue, stimulated the formation of blood vessels near the decompressed zone, enhanced the creeping substitution of the necrotic bone, eliminated the necrosis, and significantly reduced the hip pain. However, the biomechanical structure was also damaged, new stress concentration appeared, leading to trabecular microstructure fracture, weakening the mechanical strength of the femoral head, blocking the extension of the repair tissues, and delaying the repair of the subchondral bone, which in turn further affected the mechanical strength of the diseased femoral head and accelerated the process of collapse and necrosis [16–19].

Conclusions

FHISD provides good support, giving the damaged biomechanical structure chance to restore, reducing the stress concentration, and reducing the pressure and displacement of the femoral head when stress loaded.

References:

1. Van Laere C, Mulier M, Simon JP et al: Core decompression for avascular necrosis of the femoral head. *Acta Orthopaedica Belgica*, 1998; 64: 269–72
2. Johnsen SP, Sorensen HT, Lucht U et al: Patient-related predictors of implant failure after primary total hip replacement in the initial, short- and long-terms. A nationwide danish follow-up study including 36,984 patients. *J Bone Joint Surg Br*, 2006; 88: 1303–8
3. Aicher A, Heeschen C, Sasaki K et al: Low-energy shock wave for enhancing recruitment of endothelial progenitor cells: A new modality to increase efficacy of cell therapy in chronic hind limb ischemia. *Circulation*, 2006; 114: 2823–30
4. Kudo P, Dainty K, Clarfield M et al: Randomized, placebo-controlled, double-blind clinical trial evaluating the treatment of plantar fasciitis with an extracorporeal shockwave therapy (eswt) device: A north american confirmatory study. *J Orthop Res*, 2006; 24: 115–23
5. Yin TC, Wang CJ, Yang KD et al: Shockwaves enhance the osteogenic gene expression in marrow stromal cells from hips with osteonecrosis. *Chang Gung Med J*, 2011; 34: 367–74
6. Reis ND, Schwartz O, Militianu D et al: Hyperbaric oxygen therapy as a treatment for stage-i avascular necrosis of the femoral head. *J Bone Joint Surg Br*, 2003; 85: 371–75
7. Noth U, Reichert J, Reppenhagen S et al: [Cell based therapy for the treatment of femoral head necrosis]. *Der Orthopade*, 2007; 36: 466–71 [in German]
8. Gangji V, Hauzeur JP, Matos C et al: Treatment of osteonecrosis of the femoral head with implantation of autologous bone-marrow cells. A pilot study. *J Bone Joint Surg Am*, 2004; 86-A: 1153–60
9. Bartonicek J, Fric V, Skala-Rosenbaum J, Dousa P: Avascular necrosis of the femoral head in pertrochanteric fractures: A report of 8 cases and a review of the literature. *J Orthop Trauma*, 2007; 21: 229–36
10. Gangji V, Toungouz M, Hauzeur JP: Stem cell therapy for osteonecrosis of the femoral head. *Expert Opin Biol Ther*, 2005; 5: 437–42
11. Wood ML, McDowell CM, Kerstetter TL, Kelley SS: Open reduction and cementation for femoral head fracture secondary to avascular necrosis: Preliminary report. *Iowa Orthop J*, 2000; 20: 17–23
12. Castro FP Jr, Barrack RL: Core decompression and conservative treatment for avascular necrosis of the femoral head: A meta-analysis. *Am J Orthop*, 2000; 29: 187–94
13. Jones LC, Hungerford MW, Khanuja HS, Hungerford DS: Outcome measures for evaluation of treatments for osteonecrosis. *Orthop Clin North Am*, 2009; 40: 179–91

14. Rastogi S, Sankineani SR, Nag HL et al: Intralesional autologous mesenchymal stem cells in management of osteonecrosis of femur: A preliminary study. *Musculoskeletal Surg*, 2013; 97: 223–28
15. Limpaphayom N, Wilairatana V, Prasongchin P: Outcome of six millimeters core decompression in avascular necrosis of the femoral head. *J Med Assoc Thai*, 2009; 92(Suppl. 5): S12–16
16. Su R, Campbell GM, Boyd SK: Establishment of an architecture-specific experimental validation approach for finite element modeling of bone by rapid prototyping and high resolution computed tomography. *Med Eng Phys*, 2007; 29: 480–90
17. Shim VB, Pitto RP, Streicher RM et al: The use of sparse ct datasets for auto-generating accurate fe models of the femur and pelvis. *J Biomech*, 2007; 40: 26–35
18. Pierannunzii L: Endoscopic and arthroscopic assistance in femoral head core decompression. *Arthrosc Tech*, 2012; 1: e225–30
19. Shi J, Chen J, Wu J et al: Evaluation of the 3D finite element method using a tantalum rod for osteonecrosis of the femoral head. *Med Sci Monit*, 2014; 20: 2556–64